

SEISMIC RISK MAPS IN TURKEY, IRAN AND MEDITERRANEAN AREAS

SADAIKU HATTORI¹⁾

SUMMARY

Seismic risk maps for Turkey, Iran and Mediterranean areas were made by using the seismic data, attenuation models and the method of extreme value fitting. The kinds of map are the following: (i) The maximum particle velocity(kine) on the base rock and (ii) The maximum acceleration(gal) on the ground. The return periods of these maps are 50, 100 and 200 years, respectively. Until the present, the kindred seismic risk maps have been made for fourteen areas which are located in and along the active seismic zones in the world. In this paper, only some of them are shown.

1. INTRODUCTION

Many researches on the expectancy of maximum earthquake motions have been made for Japan, the United States and others (1,2,3,4,5,6,7). Hattori (8) showed the ground characteristics in the long period range(2 - 5 sec) for the whole vicinity of Japan. He gave a definition of the base rock(9), defined the temporal variations of seismicity in and around Japan using the accumulative energy curve, and proposed to express the seismic risk by combining the following three kinds of map(10): (i) Maximum earthquake motions on the base rock(S(S)), (ii) Ground characteristics(G(S)) and (iii) Temporal variations of seismicity(S(T)).

The first step for the evaluation of seismic risk, however, is to obtain regional distributions of expectations of maximum earthquake motions (S(S)) for some return periods being based on the spatial characteristics of seismicity. Especially, in order to work out countermeasures against earthquake disasters from the global point of view, it is important to make such seismic risk maps (S(S)) for many countries which are located in and along active seismic zones.

2. METHOD OF ANALYSIS

The outlines of analysis are as follows: (i) The maximum earthquake motions on the base rock or on the ground at arbitrary points are calculated for many earthquakes by using attenuation models. (ii) The expectations of the maximum earthquake motions for some return periods are estimated from the frequency distributions of the above maximum earthquake motions by utilizing the method of extreme value fitting. (iii) The regional distributions of the expectations are obtained by carrying out the same procedures for many points in the areas concerned.

2-1. SEISMIC DATA

For the areas concerned in this research, it was impossible to find reliable seismic data except NOAA-magnetic tape(11) which includes at least data during the period 1900 - 1977.

1) Head of Applied Seismology Sec., International Institute of Seismology and Earthquake Engineering, Building Research Institute.

The NOAA-magnetic tape includes four kinds of magnitude, (i) the body wave magnitude M_b , (ii) the surface wave magnitude M_s , (iii) the magnitude M which was determined by many observational organizations and (iv) the local magnitude M_L . For estimations of the maximum earthquake motions, it is desirable that a unified magnitude is used. Using all the data in the NOAA-magnetic tape, therefore, the relations among these magnitudes were investigated(12). The results are as follows:

$$\begin{aligned}
 M_s &= 1.081(\pm 0.014)M_b - 0.390(\pm 0.077); \rho = 0.699 \dots\dots\dots (2-1) \\
 M &= 1.161(\pm 0.019)M_b - 0.662(\pm 0.104); \rho = 0.723 \dots\dots\dots (2-2) \\
 M_L &= 0.862(\pm 0.017)M_b + 0.565(\pm 0.079); \rho = 0.739 \dots\dots\dots (2-3) \\
 M &= 0.853(\pm 0.015)M_s + 0.929(\pm 0.090); \rho = 0.847 \dots\dots\dots (2-4) \\
 M_L &= 0.679(\pm 0.041)M_s + 1.826(\pm 0.216); \rho = 0.751 \dots\dots\dots (2-5) \\
 M_L &= 0.860(\pm 0.024)M + 0.677(\pm 0.123); \rho = 0.913 \dots\dots\dots (2-6)
 \end{aligned}$$

The magnitudes M_b , M and M_L are transformed into M_s by Eqs. (2-1), (2-4) and (2-5), respectively. For the earthquake of which the focal depth has not been determined, the depth is assumed to be 20km. The magnitudes of earthquakes of which the epicenters were given but of which the magnitudes have not been determined, were roughly assumed to be as follows: Period 1901 - 1950 ; $M = 6.0$, Period 1951 - 1960 ; $M = 5.0$, Period 1961 - 1977 ; $M = 4.0$

2-2. ATTENUATION MODEL

The author(1,6) made the seismic risk maps for Japan and China using the attenuation model by Kanai. The same model was used also in this research, so that we can compare directly the seismic risk maps for areas concerned at present with the ones of Japan and China.

It is reasonable that the maximum earthquake motions on the ground are to be obtained taking account of the ground characteristics of each site for the input on the base rock. The seismic risk maps expressed by the maximum acceleration on the ground without regarding the ground characteristics, however, are also useful in earthquake engineering. For this purpose, an attenuation model which is the mean of attenuation models by Oliveira(12) and McGuire(13) was used.

2-3. EXPECTATIONS OF MAXIMUM EARTHQUAKE MOTIONS (1,6,14,15)

If a random variable X complies with a probability function of $G(X)$

$$G(X) = P(X \leq x) \dots\dots\dots (2-7)$$

the probability that x is equal to or larger than any of X_1, X_2, \dots, X_n is

$$\phi_n(x) = P(X_1 \leq x, X_2 \leq x, \dots, X_n \leq x) = G^n(x) \dots\dots (2-8)$$

Then, the return period $T(x)$ and the reduced variable z may be defined by the equations

$$T(x) = 1/(1 - \phi_n(x)) \dots\dots\dots (2-9)$$

$$z = -\ln[-\ln\phi_n(x)] \dots\dots\dots (2-10)$$

As the initial distribution function $G(x)$ is not known for the maximum earthquake motions at arbitrary points, the asymptotic distribution must be taken into considerations. There are three kinds of asymptotic distribution of extremes, and the first, the second and the third ones are defined by

$$\phi n^1(x) = \exp[-\exp(\alpha n(x-V))] \dots\dots\dots (2-11)$$

$$\phi n^2(x) = \exp\left[-\left(\frac{V-\epsilon}{x-\epsilon}\right)^k\right] \dots\dots\dots (2-12)$$

and

$$\phi n^3(x) = \exp\left[-\left(\frac{W-x}{W-V}\right)^k\right] \dots\dots\dots (2-13)$$

The first asymptotic distribution has no upper and lower limit for the variable x . On the other hand, the second one has a lower limit for the variable x , and in the third one an upper limit exists.

It may be reasonable that for the maximum earthquake motions at arbitrary points, an upper limit must exist. The third asymptotic distribution may be better than the first one or the second one as the probabilistic model. Therefore, defining the variable x_m by

$$x_m = \log A \max, m \dots\dots\dots (2-14)$$

where $A \max, m$ is the maximum earthquake motion at a certain point in the m -th unit period, the third asymptotic distribution is used in the present research.

The observational and theoretical reduced variables for the m -th unit period are put to be $y_m = m/(n+1)$ and z_m , respectively, where n is the total number of unit periods. The third asymptotic distribution most fit for n values of x_m may be obtained by determining the values of W (the upper limit of the maximum value), K (the shape parameter) and V (the characteristic maximum value) so as to minimize

$$\sigma = \sum_{m=1}^n (z_m - y_m)^2 \dots\dots\dots (2-15)$$

3. RESULTS OF ANALYSES

Using the seismic data in the extent of $9^\circ E - 36^\circ E$ and $29^\circ N - 49^\circ N$, analyses for Balkan were made every one degree in the latitude and in the longitude within $15^\circ E - 31^\circ E$ and $35^\circ N - 44^\circ N$. For Turkey and Iran areas, the seismic data were taken from the extents of $21^\circ E - 50^\circ E$ and $28^\circ N - 48^\circ N$, and $40^\circ E - 80^\circ E$ and $17^\circ N - 46^\circ N$, respectively. Analyses were made every half degree in the latitude and in the longitude within $26^\circ E - 45^\circ E$ and $33^\circ N - 42^\circ N$ for Turkey, and every one degree within $44^\circ E - 76^\circ E$ and $22^\circ N - 41^\circ N$ for Iran.

Figs. 1(a), 2(a) and 3(a) are the regional distributions of the maximum particle velocity on the base rock for the return periods 100 years. The contour lines are drawn by 0.5, 1, 2, 5, 10, 15, 20, 30 and 40 kine in each of figures. Figs. 1(b), 2(b) and 3(b) show the regional distributions of the maximum acceleration on the ground, of which the return period is 100 years. The contour lines are drawn by 20, 50, 100, 150, 200, 300 and 400 gal.

The regional characteristics of the seismic risk in these areas are described being based on Figs. 1(a), 2(a) and 3(a) (Maximum particle velocity

on the base rock (V_{max}). In the following, "Regions of a $kine \leq V_{max}$ " means that the value of V_{max} in the region is equal to or more than a $kine$.

Fig. 1(c), 2(c) and 3(c) are simplified seismic risk maps for practical use. These maps should be modified by countries concerned according to respective purposes.

3-1. REGIONAL CHARACTERISTICS OF THE SEISMIC RISK IN BALKAN AND THE VICINITY

Vit Karnik and Algermissen(4) have made a seismic risk map of the Balkan area, which is not always consistent with the present one. This is because of differences in the seismic data, the methods of analyses and the methods of expressing the seismic risk in both researches.

The map of Balkan includes Albania, Yugoslavia, Bulgaria, Greece and the western part of Turkey, where there are no regions of $30 \text{ kine} \leq V_{max}$.

- (I) Regions of $20 \text{ kine} \leq V_{max}$: (1) Area which includes Amorgos I., Anafi I., Thira I. and others which belong to Kiklades Is. (2) Area which lies northwest and southeast between Balli and Osmanlar in the western part of Marmara Sea and the southern vicinity.
- (II) Regions of $15 \text{ kine} \leq V_{max}$: (1) Area which includes Amorgos I., Naxos I., Thira I., Astipalea I. and others which belong to Kiklades Is. (I-(1)). (2) Area which lies northwest and southeast between Balli and Osmanlar in the western part of Marmara Sea and the southern vicinity (I-(2)). (3) Off the coast of Yenihisar in Daglari of Turkey. (4) Ocean area which lies east of Rodos I. (5) Area in and around Mesini which is located in the southern part of Peloponnisos Peninsula.

3-2. REGIONAL CHARACTERISTICS OF THE SEISMIC RISK IN TURKEY AND THE VICINITY

The map of Turkey includes Turkey, Cyprus I. and the most western part of Iran, where there are no regions of $30 \text{ kine} \leq V_{max}$. Though the descriptions on the western part of Turkey have been given on the map of Balkan, they are repeated again in this section.

- (I) Regions of $20 \text{ kine} \leq V_{max}$: (1) Area which lies northwest and southeast in the western Marmara Sea and the southern vicinity. (2) Area which lies east and west between Dereköy and Babso in Turkey.
- (II) Regions of $15 \text{ kine} \leq V_{max}$: (1) Area which lies northwest and southeast in the western Marmara Sea and the southern vicinity (I-(1)). (2) Area which lies northwest and southeast, or west and east between Bartin and Iskilip in Turkey (I-(2)). (3) Off the coast east of Rodos I. (4) Off the coast southwest of Yenihisar. (5) Gerede and Yalmanlar and the vicinity. (6) Bingöl and the vicinity.

3-3. REGIONAL CHARACTERISTICS OF THE SEISMIC RISK IN IRAN AND THE VICINITY

The map of Iran includes Iran, Afghanistan, Pakistan and a small part of USSR, where there are no regions of $30 \text{ kine} \leq V_{max}$. The descriptions on Pakistan are not given because they have been done on the map of India.

- (I) Regions of $20 \text{ kine} \leq V_{max}$: (1) Area in and around Kaskasu in USSR.
- (II) Regions of $15 \text{ kine} \leq V_{max}$: (1) Area in and around Kaskasu of USSR

and the northeastern vicinity (I-(1)). (2) Surchoh in USSR and the vicinity. (3) Kurgan-Tube in USSR and the vicinity. (4) Oavin in Iran and the vicinity.

4. CONCLUSIONS

In order to mitigate earthquake disasters or to work out countermeasures against the disasters, it is desirable that the earthquake motions due to great earthquakes in the future are estimated as exactly as possible.

As a substitute for the exact estimations of earthquake motions in the vicinity of Japan, the author proposed to use the seismic risk map(10) which is expressed by combining the following: (i) the maximum earthquake motions on the base rock which were presumed from the spatial characteristics of the seismicity in the past (S(S)), (ii) the ground characteristics which were obtained by utilizing strong motion seismograms (M(S)) and (iii) the temporal variations of the seismicity which were derived from the accumulative energy curves (S(T)).

The above first one (S(S)) is the most basic step to get a reliable seismic risk map. The present research was undertaken to make the maps of S(S) for Balkan, Turkey and Iran areas.

Two kinds of seismic risk map were made: (i) The maximum particle velocity on the base rock and (ii) The maximum acceleration on the ground.

Simple descriptions were given on the regional characteristic of the seismic risk for three areas, respectively.

A simplified map, which is convenient for practical use, was proposed for each of the areas. These kinds of proposals have already been made in Japan and the United States, and they have been utilized for the practical use of engineering. As shown in each simplified map, the seismic risk has been classified into five ranks such as A,B,C,D and E. These maps should be modified by the respective countries themselves according to each purpose.

Until the present, the similar seismic risk maps have been made fourteen areas which are located mainly along the seismic zones in the world.

ACKNOWLEDGEMENTS

The author is indebted to Mr. Hiroshi Tanaka of International Institute of Seismology and Earthquake Engineering (IISEE) who helped the author in calculating and making diagrams.

REFERENCES

- (1) HATTORI, S., 1976, Regional Distribution of presumable Maximum Earthquake Motions at the Base Rock in the Whole vicinity of Japan, Bull. IISEE, 14, 47-86.
- (2) BORGES, J. F. and RAVARA, A., 1970, "Recent Portuguese Research on Earthquake Engineering", III European Conference on Earthquake Engineering, Sofia.

- (3) LOMNITZ, C., 1969, "Earthquake Risk Map of Chile", 4th World Conference on Earthquake Engineering, Chile, 161-171.
- (4) Vit KARNIK and S. T. ALGERMISSEN, Seismic Zoning (Seismic Risk Evaluation of the Balkan Region), Report for UNDP/Unesco Survey of the Seismicity of the Balkan Region, Denver, U.S. Geological Survey.
- (5) ALGERMISSEN, S. T., and PERKINS, D. M., 1972, "A Technique for Seismic Risk Zoning, General Considerations and Parameters", Proceedings, Microzonation Conference, University of Washington, Seattle, Wash., 865-877.
- (6) HATTORI, S., 1978, Seismic Risk Maps in the world (Maximum Acceleration and Maximum Particle Velocity) (I) - China and its Vicinity, Bull. IISEE - Vol. 16, 119-150.
- (7) ESTEVA, L., 1976, Seismic risk and engineering decisions, Library of Congress Cataloging in Publication Data, Elsevier Scientific Publishing Company, Amsterdam, 179-224.
- (8) HATTORI, S., 1977, Regional Peculiarities on the Maximum Amplitudes of Earthquake Motion in Japan, Bull. IISEE, 15, 1-21.
- (9) HATTORI, S., 1977, A Proposal of the Earthquake Danger Map Based on Seismicity and Ground Characteristics, Bull. IISEE, 15, 23-32.
- (10) HATTORI, S., 1978, Temporal Variations of Seismicity and Seismic Risk in and around Japan, Bull. IISEE, 16, 105-118.
- (11) Seismic Data (Magnetic Tape) in the world, World Data Center A for Solid Earth Geophysics, U.S. Department of Commerce, National Oceanic and Atmospheric Administration Environmental Data Service (NOAA).
- (12) OLIVEIRA, C., 1974, Seismic Risk Analysis, EERC 74-1, Earthquake Engineering Research Center, University of California, Berkeley, 1-102.
- (13) MCGUIRE, R. K., 1974, Seismic Structural Response Risk Analysis incorporating peak Response Regressions on Earthquake Magnitude and Distance. Mass. Inst. Technol. Dep. Civ. Eng., R74-51.
- (14) GUMBEL, E. J., 1957 Statistics of EXTREMES, Columbia University Press, New York, (translated by Kawada, T. et al).
- (15) TUNCEL M.Y. and J. T. KUO, 1974, Statistical Prediction of the Occurrence of Maximum Magnitude Earthquakes, B.S.S.A., 64-2, 393-414.

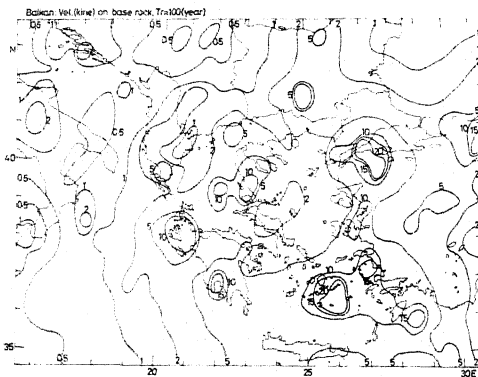


Fig. 1(a). Maximum particle velocity on the base rock in and around Balkan.

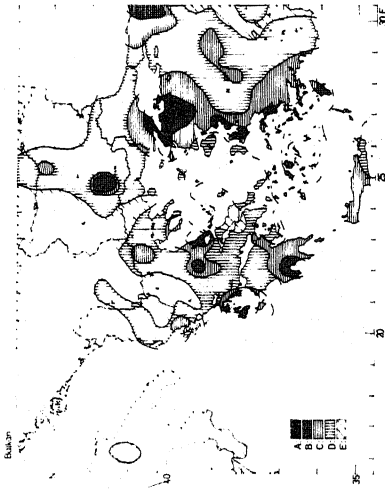


Fig. 1(c). Simplified seismic risk map in and around Balkan.

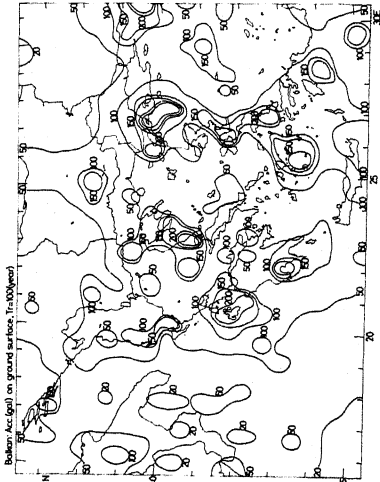


Fig. 1(b). Maximum acceleration on the ground in and around Balkan.

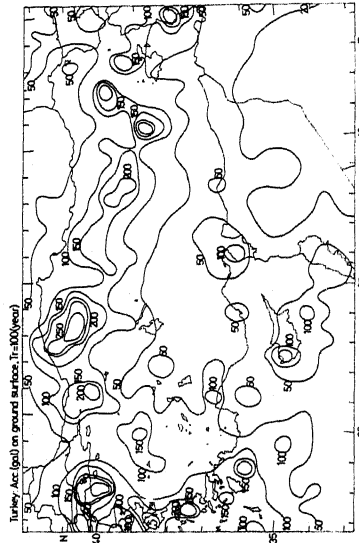


Fig. 2(b). Maximum acceleration on the ground in and around Turkey.

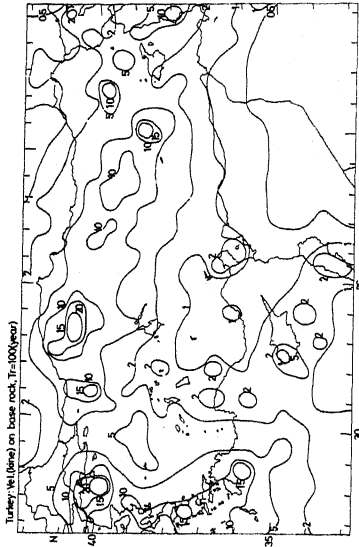


Fig. 2(a). Maximum particle velocity on the base rock in and around Turkey.

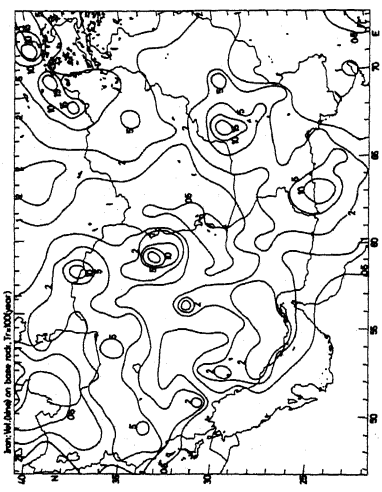


Fig. 3(a). Maximum particle velocity on the base rock in and around Iran.

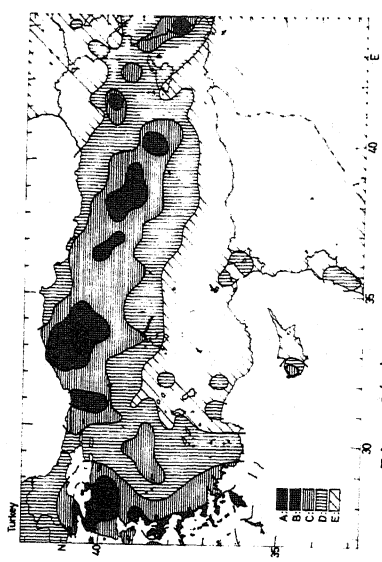


Fig. 2(c). Simplified seismic risk map in and around Turkey.

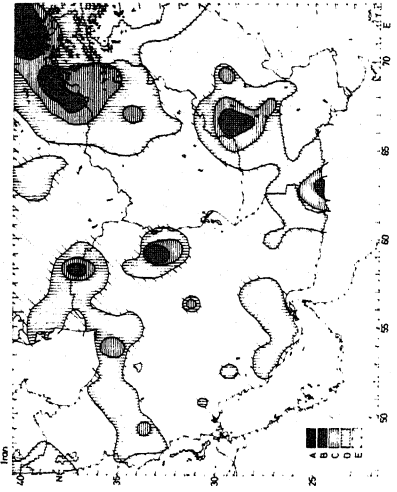


Fig. 3(c). Simplified seismic risk map in and around Iran.

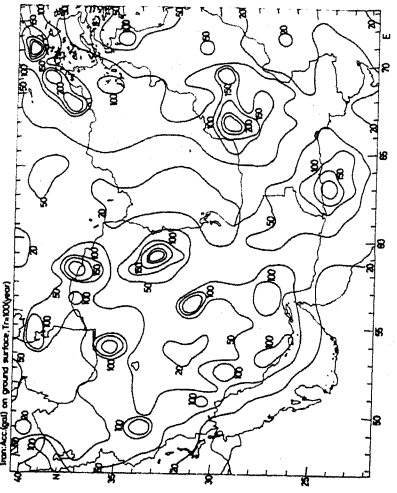


Fig. 3(b). Maximum acceleration on the ground in and around Iran.